# Three-Dimensional Surface Maps Link Local Atrophy and Fast Ripples in Human Epileptic Hippocampus

Jennifer A. Ogren, PhD,[1] Charles L. Wilson, PhD,[2,3] Anatol Bragin, PhD,[2,3] Jack J. Lin, MD,[4] Noriko Salamon, MD,[5] Rebecca A. Dutton, BS,[6] Eileen Luders, PhD,[6] Tony A. Fields, BS,[2] Itzhak Fried, MD, PhD,[7] Arthur W. Toga, PhD,[2,6] Paul M. Thompson, PhD,[2,3,6] Jerome Engel, Jr, MD, PhD,[1,2,3,8] and Richard J. Staba, PhD[2]

**Objectives:** There is compelling evidence that pathological high-frequency oscillations (HFOs), called fast ripples (FR, 150–500Hz), reflect abnormal synchronous neuronal discharges in areas responsible for seizure genesis in patients with mesial temporal lobe epilepsy (MTLE). It is hypothesized that morphological changes associated with hippocampal atrophy (HA) contribute to the generation of FR, yet there is limited evidence that hippocampal FR-generating sites correspond with local areas of atrophy.

**Methods:** Interictal HFOs were recorded from hippocampal microelectrodes in 10 patients with MTLE. Rates of FR and ripple discharge from each microelectrode were evaluated in relation to local measures of HA obtained using 3-dimensional magnetic resonance imaging (MRI) hippocampal modeling.

**Results:** Rates of FR discharge were 3 times higher in areas of significant local HA compared with rates in nonatrophic areas. Furthermore, FR occurrence correlated directly with the severity of damage in these local atrophic regions. In contrast, we found no difference in rates of ripple discharge between local atrophic and nonatrophic areas.

**Interpretation:** The proximity between local HA and microelectrode-recorded FR suggests that morphological changes such as neuron loss and synaptic reorganization may contribute to the generation of FR. Pathological HFOs, such as FR, may provide a reliable surrogate marker of abnormal neuronal excitability in hippocampal areas responsible for the generation of spontaneous seizures in patients with MTLE. Based on these data, it is possible that MRI-based measures of local HA could identify FR-generating regions, and thus provide a noninvasive means to localize epileptogenic regions in hippocampus.

Ann Neurol 2009;65:000–000

High-frequency oscillations (HFOs) >80Hz have attracted much attention for their potential role in information processing, and more recently, in neurological disease in the mammalian brain. Early studies on ripple oscillations (100–200Hz) showed that these HFOs occurred bilaterally in hippocampus and parahippocampal structures of naive rodents.[1–3] Later studies described ripples in nonhuman primates and patients with epilepsy that occurred as intermittent, brief bursts (10–100 milliseconds) in mesial temporal lobe structures, but were slightly lower in spectral frequency compared with rats (ie, 80–150Hz).[4–6] In nonprimates, and possibly humans, ripples may be associated with information transfer between hippocampus and extrahippocampal structures,[7–11] but the occurrence and function of ripples in epileptogenic regions of patients with epilepsy is unclear.[12–17]

Fast ripples (FR) are another type of HFO that are typically higher in spectral frequency than ripples, and may contain frequencies as high as 600Hz. FR are strongly associated with brain areas of epileptic seizure onset,[4,5,13,15,18,19] and sometimes occur immediately before or during the onset of mesial temporal lobe seizures.[12,20] FR are believed to reflect neuronal disturbances responsible for epileptogenicity.[21] Studies in patients with mesial temporal lobe epilepsy (MTLE) and

From the [1]Department of Neurobiology, David Geffen School of Medicine at UCLA, Los Angeles, CA; [2]Department of Neurology, David Geffen School of Medicine at UCLA, Los Angeles, CA; [3]Brain Research Institute, David Geffen School of Medicine at UCLA, Los Angeles, CA; [4]Department of Neurology, UCI School of Medicine, Irvine, CA; [5]Department of Radiology, David Geffen School of Medicine at UCLA, Los Angeles, CA; [6]Laboratory of Neuro Imaging (LONI), David Geffen School of Medicine at UCLA, Los Angeles, CA; [7]Department of Neurosurgery, David Geffen School of Medicine at UCLA, Los Angeles, CA; and [8]Department of Psychiatry and Biobehavioral Sciences, David Geffen School of Medicine at UCLA, Los Angeles, CA.

Address correspondence to Dr Richard J. Staba, Department of Neurology, David Geffen School of Medicine at UCLA, 710 Westwood Plaza, Room 2155, Los Angeles, CA 90095-7169.
E-mail: rstaba@mednet.ucla.edu

Potential conflict of interest: There are no conflicts of interest, real or apparent.

Received Oct 27, 2008, and in revised form Feb 23, 2009. Accepted for publication Mar 13, 2009.

Published online in Wiley InterScience (www.interscience.wiley.com). DOI: 10.1002/ana.21703

 
Published by Wiley-Liss, Inc., through Wiley Subscription Services

rat models of human MTLE suggest that hippocampal atrophy (HA) may be the underlying anatomical disturbance contributing to FR generation. There is evidence that reduced hippocampal volumes and lower neuron densities correlate with higher rates of FR and lower rates of ripple occurrence.[15,16,22] It is also known, however, that cell loss is often greater within specific hippocampal subfields,[23–25] and may not be distributed evenly along the anterior-posterior axis of the epileptic hippocampus.[26–28] Furthermore, FR may arise from local areas that are distributed unevenly throughout the hippocampus in epileptic rats and patients with MTLE.[29,30] It is possible, then, that areas of HA may not be in close proximity to areas supporting FR generation, which would argue against our hypothesis that morphological changes associated with HA contribute to FR generation.[16]

To evaluate the relative proximity or distance between areas of HA and FR-generating areas, we used advanced magnetic resonance imaging (MRI) analysis techniques that quantify the distribution of atrophy in hippocampal 3-dimensional (3D) reconstructed models.[27,28,31–34] Moreover, in the present study using surgical patients with medically intractable MTLE, we have extended these MRI techniques by registering the position of hippocampal intracranial microelectrodes and corresponding rates of FR and ripple occurrence on these 3D maps of HA to evaluate whether local HA are associated with areas supporting the generation of FR or ripples or both.

## Subjects and Methods

### *Patients and Electrophysiological Recordings*

Subjects were patients with medically intractable seizures of probable temporal lobe origin, who were candidates for epilepsy surgery, but required intracranial depth electrode evaluation to localize brain areas where seizures began, because results from noninvasive studies suggesting focal onsets were inconclusive. In each patient, flexible polyurethane depth electrodes (AdTech Medical Instruments, Racine, WI) were implanted bilaterally (median number of electrodes per patient: 5.0 right, 4.5 left hemisphere) in temporal and frontal lobe areas, orthogonal to the lateral skull surface, to identify brain areas generating spontaneous seizure activity (Fig 1A).[35,36] Each depth electrode was 1.3mm in diameter and consisted of 7 contacts (1.5mm length) with intercontact center-to-center spacing of 6mm, except between the 2 most distal contacts, where spacing was 3mm. Brain areas of electrographic seizure onset were identified by attending neurologists at the UCLA Seizure Disorders Center following review of multiple spontaneous, independent seizure recordings. Because the objective of this retrospective study was to evaluate HFO activity in relation to areas of hippocampal atrophy and epileptogenicity, patients included in this study had unilateral mesial temporal lobe seizure onsets, evidence of hippocampal HFOs in continuous microelectrode recordings, and a complete series of postimplant MRI scans for microelectrode localization. All patients gave their informed consent to participate in this study, which was approved by the medical institutional review board of the UCLA Office for Protection of Research Subjects.

Inserted through the lumen of each depth electrode was a bundle of 9 platinum-iridium microwires (40μm diameter; impedance, 100–300kOhm at 1kHz) that extended 3–5mm beyond the tip (Fig 1A). The 9th microwire in each bundle was uninsulated (impedance, 1–3kOhm at 1kHz), and used as a reference. For each patient, wide bandwidth (0.1Hz to 5kHz) depth electroencephalogram (EEG) was recorded from 16 microelectrodes simultaneously (10kHz sampling; 12-bit precision, R.C. Electronics, Santa Barbara, CA) during overnight polysomnographic sleep studies as part of a previous study.[15] Because the highest probability for HFO discharge in nonprimates[3,37,38] and humans[19,39] occurs during episodes of slow wave sleep, unfiltered and bandpass-filtered EEG (80–500Hz; finite impulse response filter, 513 components) from each hippocampal microelectrode (n = 72) was reviewed for HFO activity (Fig 1B, C) during a 10-minute epoch of slow wave sleep at 500ms/page in a computer display window (Run Technologies, Co., Mission Viejo, CA). For microelectrodes with evidence of HFOs (18 out of 72 microelectrodes), the entire continuous recording (median duration of recording, 4.4 hours, range, 3.0–6.1 hours) was processed using a semiautomated computer algorithm to detect and quantify HFOs.[15] Wide bandwidth EEG was bandpass filtered between 80 and 500Hz, and the root mean square (RMS) amplitude using a sliding 3-millisecond window was computed from the filtered signal. Criteria for HFO, which included visual confirmation, were as follows: consecutive RMS amplitude values >5 standard deviations (SD) above the grand mean RMS amplitude, >6 milliseconds in duration, and >6 peaks exceeding 3 SD above the overall mean amplitude of the rectified bandpass-filtered signal. Power spectral analysis (1,024-point fast Fourier transform with zero padding and Hamming window) was used to identify spectral frequency corresponding to maximum power for each HFO (Fig 1B, C). Using spectral frequency criteria from previous quantitative studies that separated human ripples and FR,[15,19] in the present study, HFOs with maximum power corresponding to a peak spectral frequency between 80 and 150Hz were labeled ripples, whereas HFOs with a peak spectral frequency between 151 and 500Hz were labeled FR. For each microelectrode that captured HFOs, a mean rate of ripple and FR discharge per minute was computed as the total number of ripples or FR divided by length of recording time.

### *Neuroimaging and Hippocampal 3D Reconstruction*

Whole brain MRI scans from patients (n = 10; 4 female; overall mean age: 35.5 ± 10.2 years) were acquired in the axial plane using a 1.5T Siemens (New York, NY) Sonata full body scanner with head coil. 3D T1-weighted images were acquired using a spoiled gradient recalled sequence (256 × 256 × 124 matrix; 1mm isotropic voxels; field of view, 28 cm; echo time, 9 milliseconds; repetition time, 40 milliseconds). Control subjects without history of neurological disease (n = 19; 6 female, mean age: 29.9 ± 3.9 years)

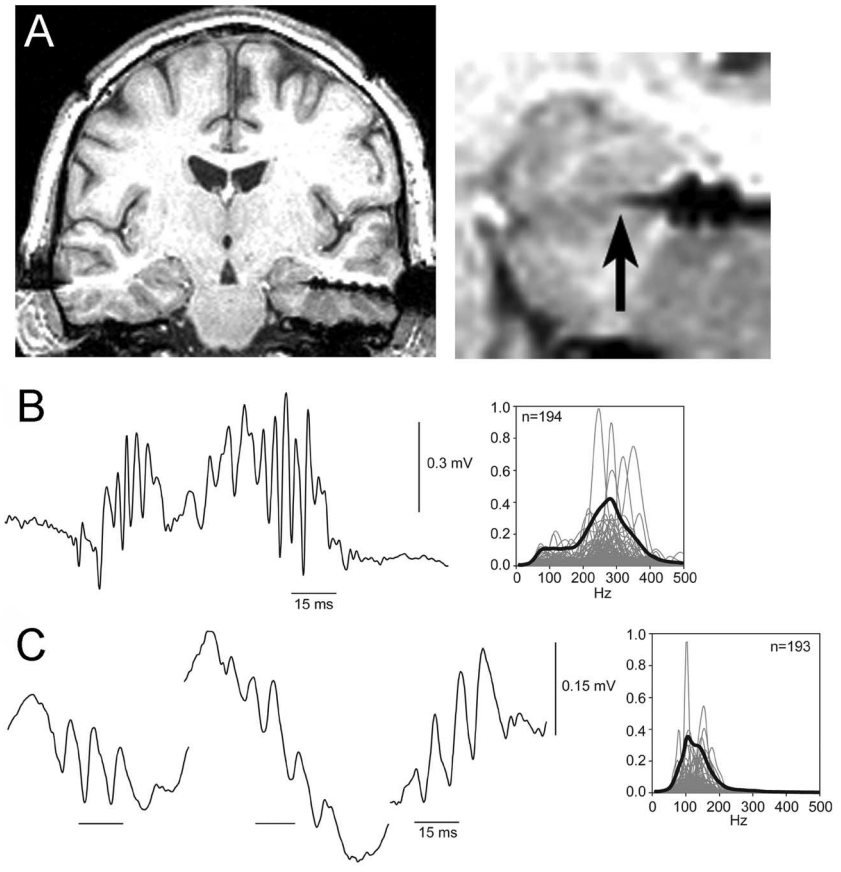


*Fig 1. Interictal high frequency oscillations recorded from microelectrodes in the human hippocampus. (A) Coronal postimplant magnetic resonance imaging (left) showing depth electrode positioned in left temporal lobe orthogonal to lateral surface of temporal bone. Note that the area of signal dropout is larger than the actual size of the depth electrode. (*Right*) Magnification of the distal end of the depth electrode showing microelectrode bundle extending beyond the tip (black arrow), and positioned in the head of the hippocampus. (B) Low pass (600Hz) filtered trace of consecutive FR discharges recorded from a different microelectrode positioned in the ipsilateral anterior hippocampus of 1 patient. To the right of this trace are results of the power spectral density (PSD) analysis using bandpass-filtered fast ripples (FR) (60–600Hz) recorded on the same microelectrode that shows normalized individual FR power (gray lines) and mean power (thick black line). FR (n = 194) recorded from this site had peak power corresponding to frequencies >200Hz (mean peak, 279Hz). (C) Examples of low pass filtered ripples recorded from a microelectrode positioned in the contralateral anterior hippocampus of a different patient. Results of PSD analysis (*right*) indicate ripples (n = 193) recorded on this microelectrode had mean peak power centered on 105Hz.*



were scanned using equivalent scan parameters on a different 1.5T MR scanner.

3D MRI scans from each subject were linearly registered to the ICBM53 (International Consortium for Brain Mapping) average brain template in a semiautomated fashion,[40] and subsequently transformed into standard space, reoriented, resampled, and resliced in the coronal plane. The dentate gyrus, hippocampus proper, presubiculum, and subiculum were identified visually on each coronal slice using a standard neuroanatomic atlas,[41] and were included in the hippocampal tracings. The boundaries of each hippocampus were delineated manually by a single experimenter blind to hemisphere of seizure onset (Fig 2A), according to criteria adapted from the Insausti and Pitkanen volumetric analysis and Laboratory of Neuro Imaging, David Geffen School of Medicine at UCLA hippocampal segmentation protocols.[42] A 3D parametric mesh model of each traced hippocampus (n = 58) was created using established hippocampal modeling methods.[27,34,43,44] Each model consisted of 30,000 points, distributed across the hippocampal surface in a spatially normalized manner.[45] The distance from each of the surface points to the medial curve, which runs through the center of the hippocampus along its longitudinal axis, is known as radial distance, and is a measure of hippocampal "thickness" (Fig 2B, C). Inter-rater reliability, based on an analysis of 10 whole hippocampal volumes traced by two investigators, was strong between investigators using the tracing protocol, with small differences in whole volume (single measurement, model 2 intraclass correlation = 0.94, F = 2.47).[44–46]

To locate each microelectrode in the 3D hippocampus, postimplant MRI was linearly registered to the same preimplant MRI that was used to construct the 3D hippocampus. The tip of the microelectrode viewed on coronal postimplant

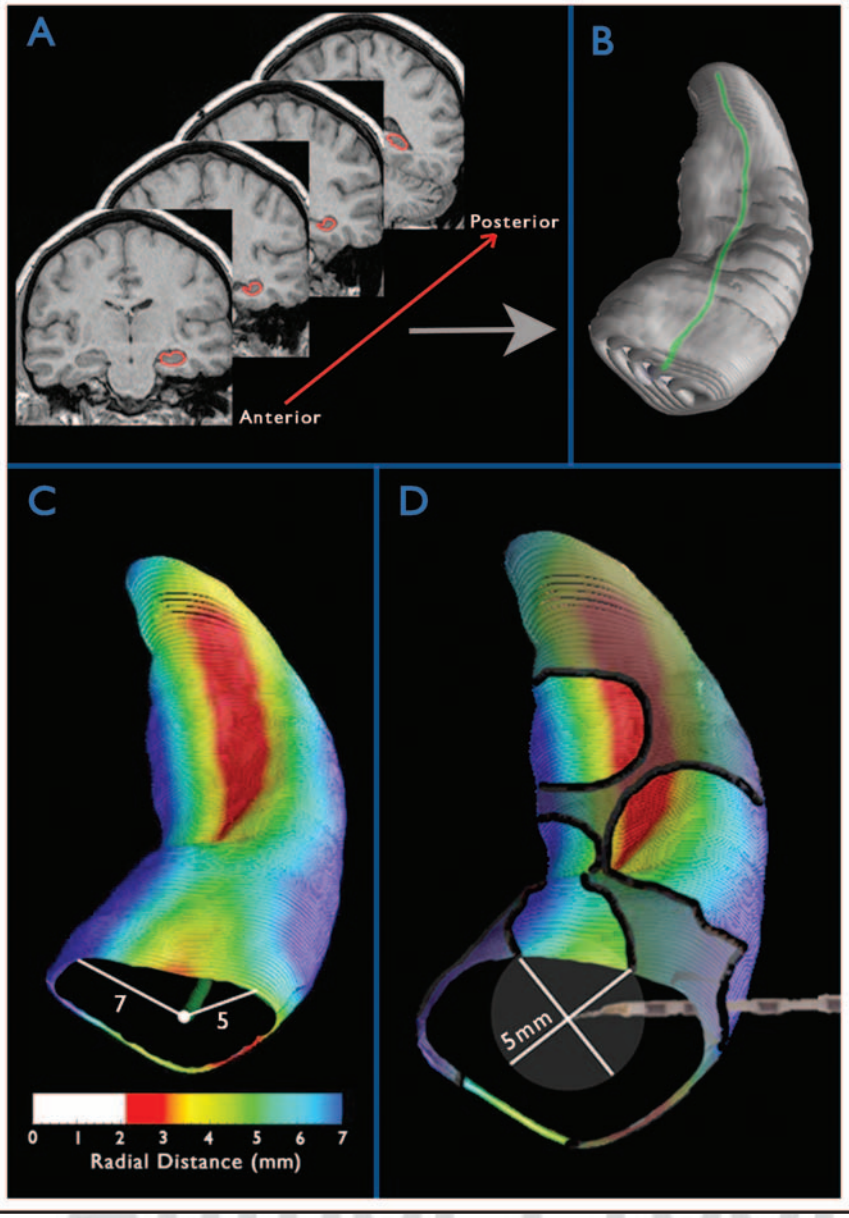


COLOR

*Fig 2. Three-dimensional (3D) hippocampal surface modeling. (A) The hippocampus is traced manually in consecutive coronal magnetic resonance imaging slices. From the hippocampal tracings, a 3D hippocampal model (B) is constructed. The medial curve (represented in green) threads through the hippocampus longitudinally, connecting hippocampal centers of mass. (C) The distance from the medial curve to the hippocampal surface (radial distance) is measured at each hippocampal surface point and mapped onto the surface model in a color-coded manner. (D) Following electrode localization in 3D space, the distance from each microelectrode tip to the hippocampal surface is measured, and surface points within 5mm of the tip were selected for subsequent analyses. Shown is an example of 1 microelectrode and corresponding surface area directly above outlined in black. Remote areas outlined in black correspond with other microelectrodes not shown.*

scans was identified (eg, Fig 1A), and the x, y, and z coordinates corresponding to the tip were registered to the 3D hippocampus. Hippocampal areas within a 5mm radius of each microelectrode tip (Fig 2D), and in a separate analysis 3mm radius, were used to evaluate hippocampal thickness in relation to HFO activity. These distances were consistent with results from previous patient studies that suggested HFOs could be recorded from distances up to 5mm,[13,20,30] and in the present study, were comparable with the overall mean radial distance of the patient hippocampus.

## Data Analysis

Patient hippocampi were separated into ipsilateral and contralateral groups based on each patient's hemisphere of ictal onset, which were compared with hippocampi from the cor-

responding hemisphere in the entire control group, which consisted of a similar proportion of male to female subjects, and similar mean age. Analysis of variance (ANOVA) was used to statistically evaluate differences in hippocampal thickness between patients and controls at each homologous surface point in relation to side of ictal onset. $p$ Values corresponding to the ANOVA F ratio at each surface point were color-coded and mapped onto the surface of 3D hippocampus to depict the distribution of statistically significant atrophy in the patient group.[27,33,45] Areas on the 3D $p$ maps corresponding to $p < 0.05$ were labeled "atrophic," whereas areas associated with $p \geq 0.05$ were labeled "nonatrophic". Permutation testing was used to correct for multiple comparisons,[47] and to determine the likelihood that the observed proportion of suprathreshold $p$ map statistics ($p < 0.01$) could occur by chance.[45,48] The number of permutations $N$ was chosen to be $1 \times 10^6$ to control for the standard error of omnibus probability $p$, which follows a binomial distribution B($N$, $p$) with known standard error.[49] The margin of error (95% confidence interval) for $p$ is approximately 5% when $N = 8{,}000$. To further improve upon this, we ran 100,000 permutations, and chose a significance level of 0.01. Microelectrode data from all patients were combined and assigned to one ipsilateral and one contralateral hippocampus. In hippocampal areas where microelectrode data overlapped from multiple patients, a distance-weighted average of rates of FR or ripple discharge, with respect to the surface, was computed. Student $t$ tests were used to compare whole hippocampal volumes within and between patient and control groups, and rates of ripple and FR occurrence in local atrophic and nonatrophic areas. In the latter analysis, the $t$ statistic was adjusted using within- and between-group correlation coefficients to compensate for the potential effects of nonindependent samples in the parametric analysis.[50,51] Correlation analysis was used to evaluate hippocampal volume reductions and magnitude of local atrophy, computed as a ratio of patient to control mean radial distance, in relation to rates of ripple and FR discharge.

## Results

Ten patients with unilateral mesial temporal lobe seizure onsets, and 19 age- and gender-matched subjects without history of neurological disorder, participated in this study. Consistent with the area of seizure onset and incidence of hippocampal sclerosis in these patients (Table), quantitative MRI analysis revealed that T1 patients had significantly smaller ipsilateral hippocampal volumes compared with control subjects (patients, mean volume ± standard error: 2,607 ± 220 mm$^3$; controls: 3,621 ± 86 mm$^3$; mean volume reduction: 29 ± 6%; $p < 0.001$), but contralateral volumes were not statistically different from controls (patients: 3,531 ± 167 mm$^3$; controls: 3,698 ± 90 mm$^3$; mean volume reduction: 4 ± 6%; $p < 0.39$). Within the patient group, ipsilateral hippocampi were 26 ± 6% smaller than hippocampi contralateral to onset ($p < 0.004$). No such asymmetry was observed within the control group (2 ± 2%, $p < 0.54$).

In patients, the mean rate of FR occurrence recorded from microelectrodes ipsilateral to seizure onset was twice as high as rates recorded contralaterally (0.42 ± 0.19 per minute vs 0.21 ± 0.15 per minute). The mean rate of ripple occurrence was 3 times higher in contralateral compared with ipsilateral hippocampi (0.12 ± 0.07 per minute vs 0.04 ± 0.02 per minute). Analysis of hippocampal volumes in relation to rates of HFO discharge revealed that greater hippocampal volume reductions correlated with higher FR rates ($r = 0.53$, $p < 0.024$). Ripple rates, however, did not cor-

***Table.*** **Patient Clinical Variables**

| Subject | Age at Surgery (yr)/ Gender/ Handedness | Age at Onset of Seizures (yr) | Seizure Frequency Prior to Depth Evaluation | Location of Seizure Onset | | Percent Hippocampal Volume Loss[a] | | Surgical Outcome | | Pathology |
|---|---|---|---|---|---|---|---|---|---|---|
| | | | | Hemisphere | Structure | Ipsilateral | Contralateral | Class[b] | Follow-up (yr) | |
| 1 | 39/F/RH | 37 | 3/mo | R | PH, PHG | 18.8 | 17.1 | N/A[c] | — | — |
| 2 | 19/F/RH | 3 | 6/wk | R | AH | 43.6 | 27.0 | I | 4.0 | HS |
| 3 | 43/M/RH | 33 | 2-3/mo | L | AM, AH | (12.4) | (8.2) | I | 4.1 | Non-HS |
| 4 | 24/M/LH | Birth | 1-2/mo | R | AH,EC | 2.9 | (13.6) | I | 3.7 | N/A[d] |
| 5 | 20/M/LH | 9 | 1/wk | L | AH, MH, EC | 41.4 | (12.6) | I | 3.3 | HS |
| 6 | 34/F/RH | 3 | 3-5/mo | R | AM, AH, MH | 39.7 | 5.3 | I | 6.6 | HS |
| 7 | 34/M/RH | Birth | 2-10/wk | R | AH | 28.6 | (11.4) | I | 3.2 | HS |
| 8 | 28/M/RH | 12 | 2+/mo | R | PH | 52.6 | 2.3 | I | 5.6 | HS |
| 9 | 39/F/RH | 3 | 2-3/mo | L | EC | 43.5 | 40.0 | III | 3.9 | HS |
| 10 | 46/M/RH | 5 | 12-15/mo | L | AM, EC | 28.0 | (2.4) | I | 5.0 | HS |

[a]Loss with respect to hemisphere- and gender-matched control subjects; percentages in parentheses denote patient volume greater than control. [b]Engel outcome classification.[57] [c]Surgery postponed for further medical evaluation. [d]Incomplete tissue specimen precluded pathological diagnosis.[58] F = female; RH = right-handed; R = right; PH = posterior hippocampus; PHG = parahippocampal gyrus; N/A = not available; AH = anterior hippocampus; M = male; LH = left-handed; HS = hippocampal sclerosis; AM = amygdala; EC = entorhinal cortex; MH = middle hippocampus.

relate significantly with reductions in hippocampal volume ($r = -0.23$, $p < 0.36$).

*Hippocampal 3D Reconstruction*

Advanced MRI-based hippocampal surface mapping techniques were used to evaluate the distribution of local HA in patients with respect to the control subjects (Fig 2). The statistical probability or $p$ maps shown in F3 Figure 3 depict areas of significant atrophy in patients ipsilateral and contralateral to ictal onset. Probability values were color coded to distinguish hippocampal areas of significant atrophy (colored white and red) from areas that were not significantly different between patient and control groups (colored yellow, green, and blue). Hippocampal $p$ maps ipsilateral to ictal onset revealed extensive atrophy distributed heterogeneously throughout the hippocampus on both superior and inferior surfaces (Fig 3, left column). Overall, these ipsilateral atrophic areas were significant after correcting for multiple comparisons ($p < .01$; see Subjects and Methods). In contrast, contralateral $p$ maps revealed a noticeably different distribution of atrophy, where HA was limited to a few circumscribed areas on the superior and inferior surfaces. Overall, the extent of atrophy depicted in contralateral $p$ maps was not significant ($p = 0.07$).

To evaluate local HA in relation to microelectrode-recorded FR and ripples, each microelectrode was registered to the respective ipsilateral or contralateral 3D hippocampus, and hippocampal areas within a 5mm radius of each microelectrode tip were outlined. Figures F4 4A and B show the surface location of these local areas, and corresponding rates of FR and ripple discharge that were recorded from each microelectrode in the AQ: 1 depth. Rates of FR and ripple discharge were color coded to distinguish microelectrodes with high (colored red) versus low (colored blue) rates of discharge, whereas areas colored gray reflect hippocampal regions >5mm from the tip of any microelectrode. Microelectrodes were more widely distributed in hippocampi ipsilateral (n = 10 sites) to seizure onset than in contralateral hippocampi (n = 8), which was a result of the placement of intracranial depth electrodes used in the clinical diagnostic evaluation of each patient's seizure disorder. Ipsilateral FR maps revealed a predominance of higher FR rates, whereas lower FR rates were observed contralaterally (Fig 4A). In contrast, ripple maps showed that higher ripple rates were more common contralateral to seizure onset (Fig 4B).

Overall, significant atrophy (ie, $p$ map areas with $p < 0.05$) accounted for 38% of total surface area within ipsilateral and contralateral hippocampal nongray areas shown in Figure 4, whereas the remaining 62% was nonatrophic (ie, $p > 0.05$). Rates of FR discharge were 94% higher in atrophic areas compared with nonatrophic areas (mean rate ± standard error: 0.58 ± 0.008 per minute vs 0.30 ± 0.004 per minute; $p < 0.001$). Furthermore, within these same atrophic regions, higher rates of FR discharge correlated directly with greater atrophy ($r = 0.65$, $p < 0.01$). In contrast, rates of ripple occurrence were not significantly different between atrophic and nonatrophic areas (0.069 ± 0.001 per minute vs 0.064 ± 0.001 per minute; $p < 0.60$).

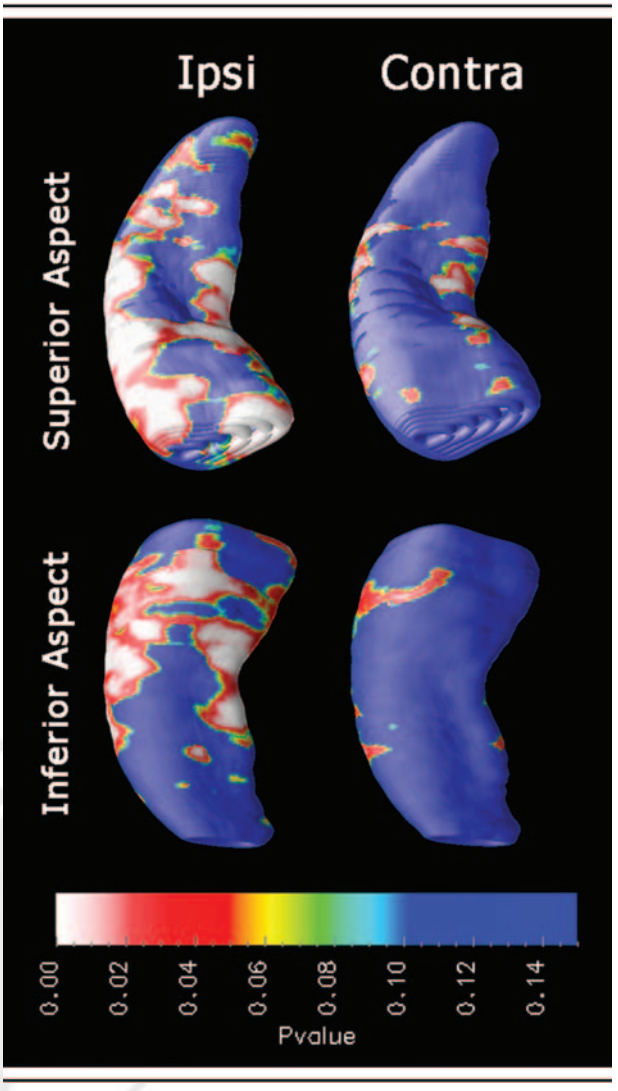


COLOR

*Fig 3. Probability or* p *maps depicting the distribution of statistically significant hippocampal atrophy in mesial temporal lobe epilepsy patients. Areas colored white and red indicate regions where patient hippocampi are significantly smaller than control hippocampi (analysis of variance [ANOVA],* $p < 0.05$*). Cooler colors (eg, green and blue) indicate regions without atrophy relative to control hippocampi (ANOVA,* $p > 0.05$*). Ipsilateral ("Ipsi,"* left column*)* p *maps display significant local atrophy in many areas on superior and inferior surfaces. Overall, the distribution of atrophy was statistical significant (*$p < 0.01$*). Contralateral ("Contra,"* right column*)* p *maps show a few isolated areas of atrophy, but when corrected for multiple comparisons, contralateral atrophy was not significant (*$p = 0.07$*).*

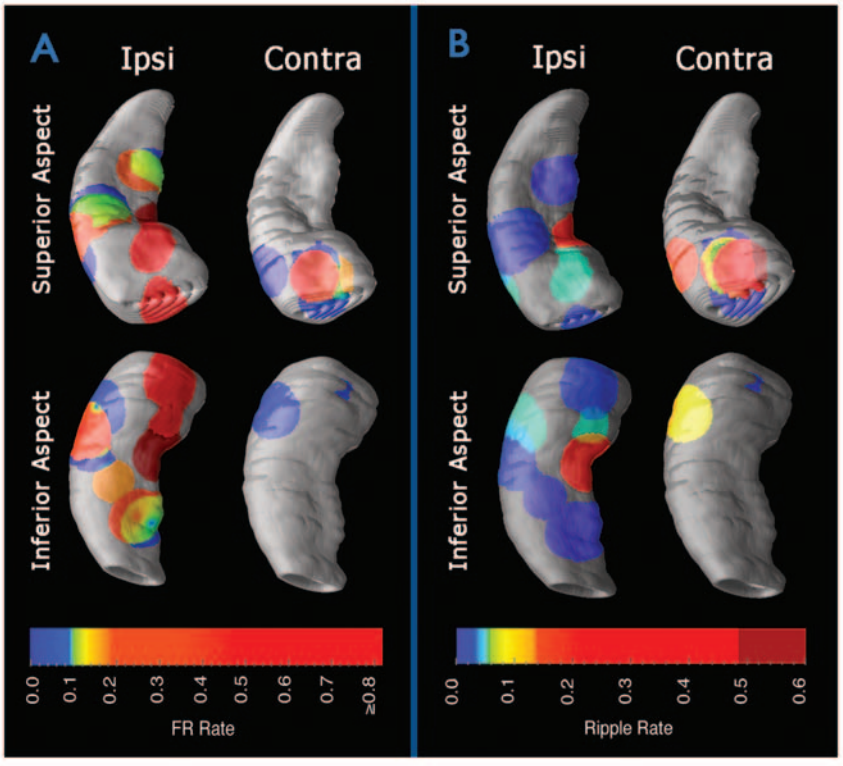


COLOR

*Fig 4. High-frequency oscillation (HFO) maps depicting rates of fast ripples (FR) and ripple occurrence (events per minute) in hippocampi of 10 patients (18 microelectrode recording sites) with mesial temporal lobe epilepsy. Maps of sites ipsilateral ("Ipsi") to seizure onset reflect HFO data recorded from 10 microelectrodes, and contralateral ("Contra") maps include HFO data from 8 microelectrodes. Hotter colors (eg, red and orange) represent higher rates of occurrence, whereas cooler colors (eg, blue and green) indicate regions where rates of occurrence are lower. (A) FR maps show a greater number of recording sites with high rates of FR occurrence in ipsilateral compared with contralateral hippocampi. In contrast, ripple maps (B) show more sites with low rates of ripple occurrence in ipsilateral hippocampi than in contralateral hippocampi. Note that the position of microelectrodes in the contralateral hippocampus overlapped to a greater extent compared with microelectrode placements in the ipsilateral hippocampus.*

In a separate analysis that examined atrophy within a radius of 3mm from each microelectrode, 43% of the total surface surrounding the microelectrodes was atrophic, and 57% was nonatrophic. Rates of FR occurrence were 182% higher in atrophic areas than in nonatrophic areas (0.73 ± 0.02 per minute vs 0.26 ± 0.007 per minute; $p < 0.001$), and correlated directly with magnitude of local atrophy ($r = 0.72$, $p < 0.01$). Analysis of ripples did not reveal any difference in rates of occurrence between atrophic and nonatrophic areas (0.084 ± 0.002 per minute vs 0.095 ± 0.002 per minute; $p < 0.72$).

## Discussion

Data from the present study extend results from previous studies that examined anatomical disturbances associated with FR and ripples, and also provide new information on the extent of HA in relation to FR and ripples. Using microelectrode-recorded data in conjunction with hippocampal surface maps, we found that the occurrence of FR was significantly higher in regions of local atrophy than in nonatrophic areas. Furthermore, within atrophic regions, higher rates of FR discharge correlated with greater atrophy. In previous studies using kainic acid (KA)-treated epileptic rats, FR were observed primarily within or adjacent to the KA-induced lesion,[29,52] but the extent of the lesion was not quantified, nor analyzed with respect to the rate of FR occurrence. Higher ratios of FR to ripple discharge have been shown to correlate with greater CA3 neuron loss in pilocarpine-treated epileptic rats,[22] and with smaller hippocampal volumes in patients with temporal lobe epilepsy,[16] but these studies did not localize atrophy or cell loss specifically near the recording electrodes, and therefore do not indicate whether FR-generating sites coincide with local areas of HA. Unlike previously used techniques, 3D surface map–based methods retain information on the spatial distribution of HA, and, when combined with the registration of microelectrodes, allowed us to examine HA within several millimeters of the microelectrode. Results from our analysis suggest that local areas of atrophy are in close proximity to sites generating FR.

It is important to note that the maps shown in Fig-

ure 4 depict local hippocampal areas of FR and ripple discharge adjacent to the microelectrodes, but likely do not represent the complete spatial distribution of FR and ripple events. So although our data clearly show that FR occurrence is significantly higher within atrophic hippocampal areas, it is not clear how well these maps reflect the actual volume of tissue supporting the generation of FR. Voltage versus depth profile analysis using microelectrodes in KA-treated epilepsy have estimated that $1mm^3$ of tissue may be sufficient to support the generation of FR,[21,29] which may or may not be the actual volume of tissue generating FR. Recordings using macroelectrodes in patients with medically refractory epilepsy suggest FR-generating areas are larger,[13,20] but how much larger is not known. The present study found a stronger correlation between rates of FR occurrence and local HA when a more conservative 3mm radius was used compared with 5mm, suggesting that human hippocampal networks generating FR may occupy a smaller volume of tissue than those represented in Figure 4. Nevertheless, the strength of 3D surface map results, which were consistent with reductions in whole volume, suggest that the resolution of our technique was sufficient to detect local atrophy and characterize atrophy with respect to rates of FR discharge.

Analysis in the present study used group atrophy data and individual FR rates, except where microelectrode recording sites overlapped across patients, in which case averaged FR rates were used. It may be somewhat unexpected, therefore, to have found a significant correlation between local HA and FR rates, given the potential variability in the distribution of atrophy between patients, and the low probability of capturing FR using fixed electrodes in any individual patient. However, a strength of the analysis is the detection of statistically significant atrophy that takes into consideration patient variability. Thus, the atrophy patterns we observed represent hippocampal areas consistently damaged across patients participating in this study. Furthermore, it is possible that in patients with MTLE who have had many years of uncontrolled seizures, there may be higher probability of capturing FR due to a larger area supporting FR or to a greater number of FR-generating sites. This explanation is consistent with studies using epileptic KA-treated rats that showed that higher rates of seizure occurrence were associated with a greater number of FR generating sites.[52] Thus, our results may also indicate a greater density of FR-generating sites in atrophic epileptogenic areas, which typically are associated with substantial neuron loss.

Following hippocampal injury, neuron loss and synaptic reorganization are implicated as the morphological changes underlying the increased propensity for neuronal synchronization and the development of chronic spontaneous seizures in the KA rat.[53] In KA-treated epileptic rats, greater neuron loss corresponds with greater axon sprouting, and likely greater synaptic organization and synchrony of discharges.[54] It is thought that synaptic reorganization leads to the abnormal formation of small clusters of neurons that fire synchronous bursts of action potentials, and that FR represent the field potentials of these neuronal events.[29] FR generating sites are widely and heterogeneously distributed, and when local inhibition decreases, evidence suggests they can enlarge, coalesce, and synchronize.[55] If a critical mass is reached, this highly synchronous bursting may result in seizure genesis. The mechanisms underlying seizure genesis proposed in these previous studies suggest interictal FR may be a surrogate marker of hippocampal regions capable of generating spontaneous seizures. Data in the present study, derived from patients with hippocampal seizures, showed areas of significant HA were associated with higher rates of FR activity, and suggests local HA may be a marker of hippocampal epileptogenicity.

Some recent patient studies have found a strong association between ripples and epileptogenic cortical and hippocampal areas,[13,14,39] whereas other patient and animal studies have found reduced rates of ripple discharge in epileptogenic hippocampus, which correlated with reduced Ammon's horn neuron densities.[16,22] In the present study, we did not find a significant relationship between HA and rates of ripple occurrence. It is possible that some of these differences may be due to the location of networks generating ripples, for example, hippocampus versus dentate gyrus or neocortex, or to the neuronal mechanisms underlying ripple generation.[56] It is likely, however, that not all ripples arise from abnormal neuronal activity. A recent patient study on hippocampal and entorhinal cortex ripples found firing patterns and phase relationships between ripples and putative pyramidal cells and interneurons that were similar to neuronal discharge patterns that occur during ripples generated in CA1 of naive rats.[17]

We can conclude, however, that there is a strong association between the distribution of local HA and FR discharges. FR may be a surrogate marker of areas associated with neuron loss and synaptic reorganization that contributes to hippocampal seizures in MTLE. Finally, 3D surface maps of local HA could, in turn, constitute a biomarker of FR-generating sites, which could provide a noninvasive way to localize epileptogenic hippocampal regions.

This work was supported by the National Institutes of Health NS-02808 and NS-33310. AQ: 2

We thank Dr. Gary Mathern, Eric Behnke, Tom Karnesi, and Marina Barysheva for their assistance with this study.

## References


1. O'Keefe J, Nadel L. The Hippocampus As a Cognitive Map. Oxford, UK: Clarendon Press; 1978.
2. Suzuki SS, Smith GK. Spontaneous EEG spikes in the normal hippocampus. II. Relations to synchronous burst discharges. Electroencephalogr Clin Neurophysiol 1988;69:532–540.
3. Buzsaki G, Horvath Z, Urioste R, et al. High-frequency network oscillation in the hippocampus. Science 1992;256: 1025–1027.
4. Bragin A, Engel J Jr, Wilson CL, et al. High-frequency oscillations in human brain. Hippocampus 1999;9:137–142.
5. Bragin A, Engel J Jr, Wilson CL, et al. Electrophysiologic analysis of a chronic seizure model after unilateral hippocampal KA injection. Epilepsia 1999;40:1210–1221.
6. Skaggs WE, McNaughton BL, Permenter M, et al. EEG sharp waves and sparse ensemble unit activity in the macaque hippocampus. J Neurophysiol 2007;98:898–910.
7. Siapas AG, Wilson MA. Coordinated interactions between hippocampal ripples and cortical spindles during slow-wave sleep. Neuron 1998;21:1123–1128.
8. Sirota A, Csicsvari J, Buhl D, Buzsaki G. Communication between neocortex and hippocampus during sleep in rodents. Proc Natl Acad Sci U S A 2003;100:2065–2069.
9. Molle M, Yeshenko O, Marshall L, et al. Hippocampal sharp wave-ripples linked to slow oscillations in rat slow-wave sleep. J Neurophysiol 2006;96:62–70.
10. Isomura Y, Sirota A, Ozen S, et al. Integration and segregation of activity in entorhinal-hippocampal subregions by neocortical slow oscillations. Neuron 2006;52:871–882.
11. Axmacher N, Elger CE, Fell J. ripples in the medial temporal lobe are relevant for human memory consolidation. Brain 2008; 131:1806–1817.
12. Jirsch JD, Urrestarazu E, LeVan P, et al. High-frequency oscillations during human focal seizures. Brain 2006;129: 1593–1608.
13. Urrestarazu E, Chander R, Dubeau F, Gotman J. Interictal high-frequency oscillations (100-500 Hz) in the intracerebral EEG of epileptic patients. Brain 2007;130:2354–2366.
14. Worrell GA, Gardner AB, Stead SM, et al. High-frequency oscillations in human temporal lobe: simultaneous microwire and clinical macroelectrode recordings. Brain 2008;131:928–937.
15. Staba RJ, Wilson CL, Bragin A, et al. Quantitative analysis of high-frequency oscillations (80-500 Hz) recorded in human epileptic hippocampus and entorhinal cortex. J Neurophysiol 2002;88:1743–1752.
16. Staba RJ, Frighetto L, Behnke EJ, et al. Increased fast ripple to ripple ratios correlate with reduced hippocampal volumes and neuron loss in temporal lobe epilepsy patients. Epilepsia 2007; 48:2130–2138.
17. Le Van Quyen M, Bragin A, Staba R, et al. Cell type-specific firing during ripple oscillations in the hippocampal formation of humans. J Neurosci 2008;28:6104–6110.
18. Jacobs J, LeVan P, Chander R, et al. Interictal high-frequency oscillations (80-500 Hz) are an indicator of seizure onset areas independent of spikes in the human epileptic brain. Epilepsia 2008;49:1893–1907.
19. Staba RJ, Wilson CL, Bragin A, et al. High-frequency oscillations recorded in human medial temporal lobe during sleep. Ann Neurol 2004;56:108–115.
20. Khosravani H, Mehrotra N, Rigby M, et al. Spatial localization and time-dependant changes of electrographic high frequency oscillations in human temporal lobe epilepsy. Epilepsia 2008 [Epub ahead of print]. AQ: 3
21. Bragin A, Wilson CL, Engel J Jr. Chronic epileptogenesis requires development of a network of pathologically interconnected neuron clusters: a hypothesis. Epilepsia 2000;41(suppl 6):S144–S152.
22. Foffani G, Uzcategui YG, Gal B, Menendez de la Prida L. Reduced spike-timing reliability correlates with the emergence of fast ripples in the rat epileptic hippocampus. Neuron 2007;55: 930–941.
23. Bratz E. Ammonshornbefunde bei epileptikern. Arch Psychiatr Nervenkr 1899;31:820–835.
24. Mathern GW, Pretorius JK, Babb TL. Quantified patterns of mossy fiber sprouting and neuron densities in hippocampal and lesional seizures. J Neurosurg 1995;82:211–219.
25. Sommer W. Die Erkrankung des Ammonshorns als aetiologisches Moment der Epilepsie. Arch Psychiatr Nervenkr 1880;10: 631–675.
26. Babb TL, Brown WJ, Pretorius J, et al. Temporal lobe volumetric cell densities in temporal lobe epilepsy. Epilepsia 1984; 25:729–740.
27. Lin JJ, Salamon N, Dutton RA, et al. Three-dimensional preoperative maps of hippocampal atrophy predict surgical outcomes in temporal lobe epilepsy. Neurology 2005;65: 1094–1097.
28. Ogren JA, Bragin A, Wilson CL, et al. Three-dimensional hippocampal atrophy maps distinguish two common temporal lobe seizure-onset patterns. Epilepsia 2008; [Epub ahead of print].
29. Bragin A, Mody I, Wilson CL, Engel J Jr. Local generation of fast ripples in epileptic brain. J Neurosci 2002;22:2012–2021.
30. Bragin A, Wilson CL, Staba RJ, et al. Interictal high-frequency oscillations (80-500 Hz) in the human epileptic brain: entorhinal cortex. Ann Neurol 2002;52:407–415.
31. Apostolova LG, Dinov ID, Dutton RA, et al. 3D comparison of hippocampal atrophy in amnestic mild cognitive impairment and Alzheimer's disease. Brain 2006;129:2867–2873.
32. Bearden CE, Thompson PM, Dutton RA, et al. Three-dimensional mapping of hippocampal anatomy in unmedicated and lithium-treated patients with bipolar disorder. Neuropsychopharmacology 2008;33:1229–1238.
33. Narr KL, Thompson PM, Szeszko P, et al. Regional specificity of hippocampal volume reductions in first-episode schizophrenia. Neuroimage 2004;21:1563–1575.
34. Thompson PM, Schwartz C, Toga AW. High-resolution random mesh algorithms for creating a probabilistic 3D surface atlas of the human brain. Neuroimage 1996;3:19–34.
35. Engel J Jr. Fundamental Mechanisms of Human Brain Function: Surgical Treatment of Epilepsy as an Investigative Resource. New York, NY: Raven Press; 1987.
36. Engel J Jr. Surgery for seizures. N Engl J Med 1996;334: 647–652.
37. Ylinen A, Bragin A, Nadasdy Z, et al. Sharp wave-associated high-frequency oscillation (200 Hz) in the intact hippocampus: network and intracellular mechanisms. J Neurosci 1995;15: 30–46.
38. Chrobak JJ, Buzsaki G. High-frequency oscillations in the output networks of the hippocampal-entorhinal axis of the freely behaving rat. J Neurosci 1996;16:3056–3066.
39. Bagshaw AP, Jacobs J, Levan P, et al. Effect of sleep stage on interictal high-frequency oscillations recorded from depth macroelectrodes in patients with focal epilepsy. Epilepsia 2008 [Epub ahead of print].
40. Collins DL, Neelin P, Peters TM, Evans AC. Automatic 3D intersubject registration of MR volumetric data in standardized Talairach space. J Comput Assist Tomogr 1994;18:192–205.

41. Mai JK, Assheuer J, Paxinos G. Atlas of the Human Brain. San Diego, CA: Academic Press; 1997.
42. Insausti R, Juottonen K, Soininen H, et al. MR volumetric analysis of the human entorhinal, perirhinal, and temporopolar cortices. AJNR Am J Neuroradiol 1998;19:659–671.
43. Thompson PM, Apostolova LG. Computational anatomical methods as applied to ageing and dementia. Br J Radiol 2007; 80:S78–S91.
44. Narr KL, Thompson PM, Sharma T, et al. Three-dimensional mapping of temporo-limbic regions and the lateral ventricles in schizophrenia: gender effects. Biol Psychiatry 2001;50:84–97.
45. Thompson PM, Hayashi KM, De Zubicaray GI, et al. Mapping hippocampal and ventricular change in Alzheimer disease. Neuroimage 2004;22:1754–1766.
46. Portney LG, Watkins MP. Foundations of Clinical Research: Applications to Practice. 3rd ed. Upper Saddle River, NJ: Pearson/Prentice Hall; 2008.
47. Nichols TE, Holmes AP. Nonparametric permutation tests for functional neuroimaging: a primer with examples. Hum Brain Mapp 2002;15:1–25.
48. Chiang MC, Reiss AL, Lee AD, et al. 3D pattern of brain abnormalities in Williams syndrome visualized using tensor-based morphometry. Neuroimage 2007;36:1096–1109.
49. Edgington ES. Randomization Tests. 3rd ed. New York, NY: M. Dekker; 1995.
50. Snijders TAB, Bosker RJ. Multilevel Analysis: An Introduction to Basic and Advanced Multilevel Modeling. Thousand Oaks, CA: Sage Publications; 1999.
51. Zimmerman DW, Williams RH, Zurabo BD. Effect of non-independence of sample observations on some parametric and nonparametric statistical tests. Commun Stat Simul Comput 1993;22:779–789.
52. Bragin A, Wilson CL, Engel J Jr. Spatial stability over time of brain areas generating fast ripples in the epileptic rat. Epilepsia 2003;44:1233–1237.
53. Mathern GW, Cifuentes F, Leite JP, et al. Hippocampal EEG excitability and chronic spontaneous seizures are associated with aberrant synaptic reorganization in the rat intrahippocampal kainate model. Electroencephalogr Clin Neurophysiol 1993;87: 326–339.
54. Buckmaster PS, Dudek FE. Neuron loss, granule cell axon reorganization, and functional changes in the dentate gyrus of epileptic kainate-treated rats. J Comp Neurol 1997;385: 385–404.
55. Bragin A, Azizyan A, Almajano J, et al. Analysis of chronic seizure onsets after intrahippocampal kainic acid injection in freely moving rats. Epilepsia 2005;46:1592–1598.
56. Engel JJ, Bragin A, Staba R, Mody I. High-frequency oscillations: what is normal and what is not? Epilepsia 2008; [Epub ahead of print].
57. Engel J Jr. Surgical Treatment of the Epilepsies. 2nd ed. New York, NY: Raven Press; 1993.
58. Mathern GW, Babb TL, Vickrey BG, et al. Traumatic compared to non-traumatic clinical-pathologic associations in temporal lobe epilepsy. Epilepsy Res 1994;19:129–139.